International Journal of Radiation Oncology biology • physics

www.redjournal.org

Biology Contribution

Experimental Platform for Ultra-high Dose Rate FLASH Irradiation of Small Animals Using a Clinical Linear Accelerator

Emil Schüler, PhD,* Stefania Trovati, PhD,* Gregory King, PhD,* Frederick Lartey, PhD,* Marjan Rafat, PhD,* Manuel Villegas,* A. Joe Praxel,* Billy W. Loo, Jr, MD, PhD,*,† and Peter G. Maxim, PhD*,†

Department of Radiation Oncology and †Stanford Cancer Institute, Stanford University School of Medicine, Stanford, California

Received Jun 16, 2016, and in revised form Aug 15, 2016. Accepted for publication Sep 14, 2016.

Summary

A key factor limiting the effectiveness of radiation therapy is normal tissue toxicity, and recent preclinical data have shown that ultra-high dose rate irradiation (>50 Gy/s, "FLASH") potentially mitigates this effect. However, research in this field has been strongly limited by the availability of FLASH irradiators suitable for small animal experiments. We present an

Purpose: A key factor limiting the effectiveness of radiation therapy is normal tissue toxicity, and recent preclinical data have shown that ultra-high dose rate irradiation (>50 Gy/s, "FLASH") potentially mitigates this effect. However, research in this field has been strongly limited by the availability of FLASH irradiators suitable for small animal experiments. We present a simple methodologic approach for FLASH electron small animal irradiation with a clinically available linear accelerator (LINAC).

Methods and Materials: We investigated the FLASH irradiation potential of a Varian Clinac 21EX in both clinical mode and after tuning of the LINAC. We performed detailed FLUKA Monte Carlo and experimental dosimetric characterization at multiple experimental locations within the LINAC head.

Results: Average dose rates of ≤74 Gy/s were achieved in clinical mode, and the dose rate after tuning exceeded 900 Gy/s. We obtained 220 Gy/s at 1-cm depth for a >4-cm field size with 90% homogeneity throughout a 2-cm-thick volume.

Conclusions: We present an approach for using a clinical LINAC for FLASH irradiation. We obtained dose rates exceeding 200 Gy/s after simple tuning of the LINAC,

Reprint requests to: Peter G. Maxim, PhD, Department of Radiation Oncology, Stanford University School of Medicine, Stanford Cancer Institute, 875 Blake Wilbur Dr, Stanford, CA 94305-5847. Tel: (650) 724-3018; E-mail: PMaxim@stanford.edu or Billy W. Loo, Jr, MD, PhD, Department of Radiation Oncology, Stanford University School of Medicine, Stanford Cancer Institute, 875 Blake Wilbur Dr, Stanford, CA 94305-5847. Tel: (650) 736-7143; E-mail: BWLoo@stanford.edu

Drs Schüler and Trovati contributed equally to this work.

Conflict of interest: none.

Supplementary material for this article can be found at www.redjournal.org.

Acknowledgments—The authors would like to thank Miguel Jimenez, James Clayton, Flavio Poehlmann, and Daniel Pawlak from Varian Medical Systems for their technical assistance throughout the project. The authors would also like to thank the following for financial support of this research: The Swedish Childhood Cancer Foundation, The American Association for Cancer Research, The Foundation BLANCEFLOR Boncompagni Ludovisi n'ee Bildt, The Weston Havens Foundation, the Wallace H Coulter Foundation, the Department of Radiation Oncology (Stanford University), the Office of the Dean (School of Medicine, Stanford University), the Office of the Provost (Stanford University) and SLAC National Accelerator Laboratory.

Int J Radiation Oncol Biol Phys, Vol. 97, No. 1, pp. 195–203, 2017
0360-3016/$ - see front matter © 2016 Elsevier Inc. All rights reserved.
http://dx.doi.org/10.1016/j.ijrobp.2016.09.018

experimental platform using a clinical linear accelerator capable of delivering FLASH irradiation in excess of 200 Gy/s with excellent dosimetric properties.

with excellent dosimetric properties for small animal experiments. This will allow for increased availability of FLASH irradiation to the general research community.
© 2016 Elsevier Inc. All rights reserved.

Introduction

The use of very high dose rate treatments in radiation therapy is steadily increasing owing to the technical developments and implementations in recent years (1). Techniques such as flattening filter free beams allows for up to 4 times faster treatment compared with standard irradiation protocols (1), with average dose rates of up to 0.5 Gy/s and instantaneous dose rates of $>1.7 \times 10^4$ Gy/s within a pulse (2). In proton therapy with pencil beam scanning, average dose rates of up to 200 Gy/s within a Bragg peak are readily available. The use of these high dose rate treatments has, however, raised concern about the possible radiobiologic consequences affecting the overall response to therapy.

Early studies conducted in the field of very high and ultra-high dose rate irradiation have occurred in an in vitro setting, primarily because of technical difficulties with delivering such dose rates with field sizes large enough for animal irradiation. These in vitro studies have shown little or no differential effect between ultra-high dose rate and conventional irradiation (1, 3-8). However, recent results using dose rates in the range of 40 to 60 Gy/s (FLASH) in the in vivo setting have been markedly different. In those studies, FLASH irradiation of lung tissue showed clear benefits, with reduced normal tissue toxicity but keeping the tumor response constant (9). The underlying mechanism for this response is unknown, and more research is clearly needed.

To study these effects, FLASH irradiators with the capability of delivering dose rates of >50 Gy/s need to become more accessible to the general research community. Previously developed small animal irradiation systems have primarily focused on the use of x-ray tubes or high activity radionuclide sources for the delivery of the prescribed dose (10-13). With these techniques, highly conformal dose distributions are available; however, the high dose rates needed for FLASH exposures are not practical. Furthermore, x-ray or gamma irradiation in the megavoltage range gives a highly heterogeneous dose distribution in small animals because of the substantial build-up effects. Instead, electrons in the megaelectron volt range could be used owing to the greatly decreased dose build up and a more homogeneous dose with depth in the mouse setting when using single beam irradiation (14).

In the present study, we describe a technique for using a clinical linear accelerator (LINAC) for electron FLASH irradiation of small animals. Our system has the advantage of being an adaptation of an existing commercial device with easy set up and without the risk of disturbing normal clinical operations. Furthermore, the beam energy permits a more homogeneous depth dose than the systems used to date. A dosimetric characterization and Monte Carlo (MC) simulations are presented for 2 states of the machine: with normal clinical operation settings and after tuning for maximum dose rate delivery.

Methods and Materials

A Varian Clinac 21EX (Varian Medical Systems, Palo Alto, CA) was used to investigate the high dose rate potential of a clinical LINAC. Three locations within the head of the machine were assessed for small animal irradiation: the ion chamber, positioning mirror, and inner jaws (Y jaws; Fig. 1). During the assessments, the gantry was at a 180° angle (beam directed vertically up; Fig. 1A).

Film dosimetry

The field characteristics such as beam profile and depth dose were measured using Gafchromic EBT2 films (Ashland Inc, Covington, KY). In clinical mode, the electron energies of 9 and 20 MeV were investigated with maximum dose rate settings, corresponding to ~2500 (in high dose total skin electron [HDTSE] mode) and 1000 MU/min at reference conditions (at dose maximum, Source to Surface Distance (SSD) = 100 cm) for the 9- and 20-MeV electron beams, respectively. The films were positioned between polystyrene slabs at a depth of 0, 0.5, 1, 1.5, and 2 cm at the position of the ion chamber, at the center of the positioning mirror, or at the inner jaws (Fig. 1). The total thickness of the phantom was 2.5 cm. Three independent measurements were taken at each position. No collimation of the beam was implemented during these measurements. The films were scanned 24 hours after exposure using a Perfection V500 flatbed scanner (Epson, Long Beach, CA) with 72-dpi resolution, and the net optical density was calculated. Calibration films were generated with a 16-MeV electron beam at the dose maximum depth, with 100-cm SSD and a 15×15−cm field size. Output measurements of 50 to 5000 MU were generated, and the net optical density data were fitted to a 5 degree polynomial fit.

MC simulations

A realistic geometry of the Varian Clinac 21EX was modeled in a set of simulations performed with the MC

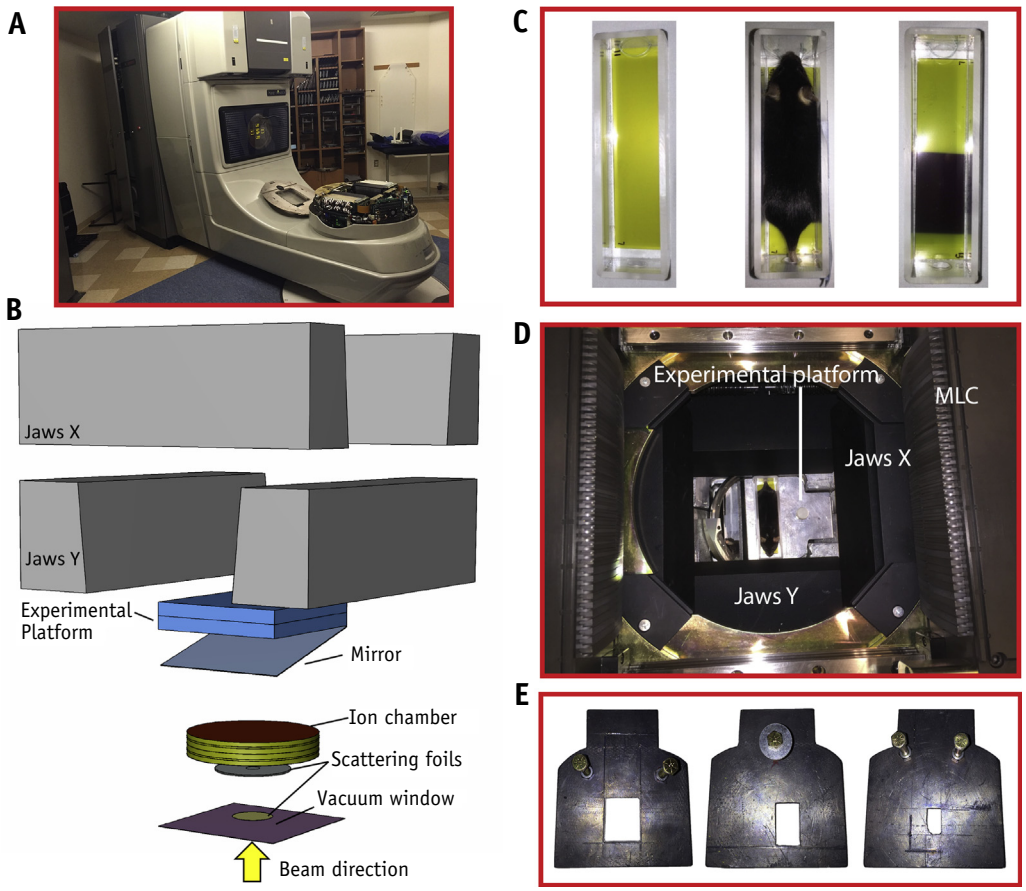

Fig. 1. The field characteristics were determined at the position of the ion chamber, mirror, and inner jaws (Y jaws). (A) Photograph of the Varian Clinac 21EX in the 180° position, (B) generated Monte Carlo geometry model of the head of the linear accelerator, (C) animal jig used for mouse immobilization and setup, (D) photograph into the head of the linear accelerator with lead sheets and animal jig at the position of the mirror, and (E) 10-mm-thick lead sheets used for abdomen, thorax, and brain irradiation. *Abbreviation:* MLC = multileaf collimator.

code FLUKA (15, 16). The created geometry included all the components that interact with the beam (ie, the vacuum window, scattering foils, ionization chamber, mirror, and jaws; Fig. 1B, Supplementary Table 1 (17)). The generated model was verified against the experimental data and was then used to evaluate the potential modifications for exploring new machine layouts. Also, the effect of the increased dose rate and its impact on the ion chamber was investigated.

Animal setup

At the position of the mirror, platforms were constructed for animal irradiation (Figs. 1D and 1E). Platforms were constructed with built-in collimation for abdomen, thorax, and brain irradiation, and the platforms were made from 10-mm-thick lead. Furthermore, an animal immobilization device (animal jig) was constructed to position the mouse with good reproducibility relative to the collimator platforms (Fig. 1C). Images from kilovoltage x-ray simulation of the fields were taken using a Spectral Ami-X imaging platform (Spectral Instruments Imaging, Tucson, AZ) using C57BL/6 mice (Charles River, Wilmington, MA). All animal procedures where approved by the Stanford University Institutional Animal Care and Use Committee (IACUC).

Tuning

Tuning of the LINAC required the use of a spare 20-MeV program printed circuit board (Varian Medical Systems), which was used to custom configure the control parameters, including the pulse forming network voltage, injector current, dosimetry calibration, and beam steering. The standard 20-MeV program printed circuit board was removed to preserve the clinical settings, and clinical treatments on the LINAC were halted for the entire duration of the experiments and until after a full annual quality assurance procedure had been completed to verify the clinical performance parameters. The waveform characteristics, including the gun pulse waveform and the automatic frequency controller trigger pulse, were measured using by an oscilloscope (Rigol, Beijing, China).

To allow for proper tuning, the dosimetry and positioning servos were disabled owing to the saturation effects in the internal ion chamber. The beam tuning used pulse repetition rate setting 1 as the starting point (Table E2; available online at www.redjournal.org). Once tuned, the dose rate could be further scaled in a straightforward way by setting a different repetition rate. The LINAC was turned on, and the gun current and radiofrequency driver were manually adjusted to find the maximum dose rate. Verification of the dose/pulse and field characteristics were performed by pinpoint ion chamber (PTW, Freiburg, Germany) and Gafchromic film, as described previously.

The beam was controlled using an Arduino Uno microcontroller (Arduino Uno; available at http://arduino.cc/en/Main/ArduinoBoardUno) connected to the gating interface, which allowed for a consistent and repeatable near-real-time control of the LINAC (Fig. E1; available online at www.redjournal.org). The Arduino Uno was programmed to open or close a dry-reed relay to switch the gating control on or off.

Results

Field characteristics

The field characteristics in the clinical setting were investigated for 2 energies (9 and 20 MeV) at 3 different positions: the ion chamber, mirror, and inner jaws. The dose rate decreased from 74 Gy/s to 5.5 Gy/s at 1-cm depth when moving from the position of the ion chamber to the position of the inner jaws for the 9-MeV HDTSE electron beam (Table 1). A similar percentage of reduction was also found for the 20-MeV electron beam. With an increased distance from the virtual source position, both the 90% and 50% field diameter increased (Table 1 and Fig. 2A-F).

The percentage depth dose (PDD) was relatively similar for the 2 energies (Figs. 2G and 2H). At the position of the inner jaws, the PDD increased slightly or remained constant with depth for 9 and 20 MeV, respectively. At the position of the mirror, the PDD decreased only slightly with depth for both energies. At the position of the ion chamber, rapid dose falloff occurred, with >30% reduction in dose at the 2-cm depth compared with the surface dose. This identified the position of the mirror as optimal for evaluating the dosimetry of organ-specific shielding.

MC results

MC simulations were performed for the 9- and 20-MeV electron beams, and the dose profiles were recorded at the position of the ion chamber, mirror, and inner jaws. The comparison between the simulated and experimental data showed full agreement for all energies and distances from the virtual source, validating the geometry model used for all MC simulations (Fig. 2A-F).

In the simulations for the modified layout, the scattering foils for the 9-MeV beam were used with a 20-MeV beam. The results showed that a marked increase in the dose rate could be achieved using scattering foils with a thinner thickness (Fig. 3A and Table E1; available online at www.redjournal.org). A dose rate increase of >300% was found, with the energy deposited (W/cm^3) in the entrance window of the ion chamber only increased by 25% (Figs. 3B and 3C). However, the usable field size was drastically reduced.

Organ-specific shielding

The field characteristics when applying shielding to irradiate specific volumes showed flat profiles for all 3 field sizes at the position of the mirror (Fig. 4). The PDD was affected by applying lead sheets, and for the abdomen and

Table 1 Dose rates and field dimensions

Position	Average dose rate (Gy/s)	Instantaneous dose rate (Gy/s)*	Field diameter (mm)	
			90%	50%
Ion chamber				
9-MeV HDTSE (400 nA)†	74 ± 0.66	82,000 ± 730	9.6 ± 0.23	36 ± 0.35
20 MeV (110 nA)	22 ± 0.24	25,000 ± 260	11 ± 0.51	33 ± 0.17
Mirror				
9 MeV HDTSE (400 nA)	15 ± 0.54	17,000 ± 600	49 ± 1.2	77 ± 1.1
20 MeV (110 nA)	5.4 ± 0.04	6000 ± 48	46 ± 1.4	65 ± 0.40
Inner jaws				
9 MeV HDTSE (400 nA)	5.5 ± 0.085	6100 ± 95	74 ± 3.1	
20 MeV (110 nA)	1.8 ± 0.026	2000 ± 29	82 ± 2.0	

Abbreviation: HDTSE = high dose total skin electron.

Measured dose rates and field dimensions at 1-cm depth at the position of the ion chamber, mirror, and inner jaws. The highest dose rates were found at the ion chamber using 9-MeV HDTSE (400 nA average current). Decreased dose rates and increased field sizes were found at the more distant levels (mirror and inner jaws).

* Instantaneous dose rate determined from measured average dose rate with 5-μs pulse length (180 Hz).

† Average current.

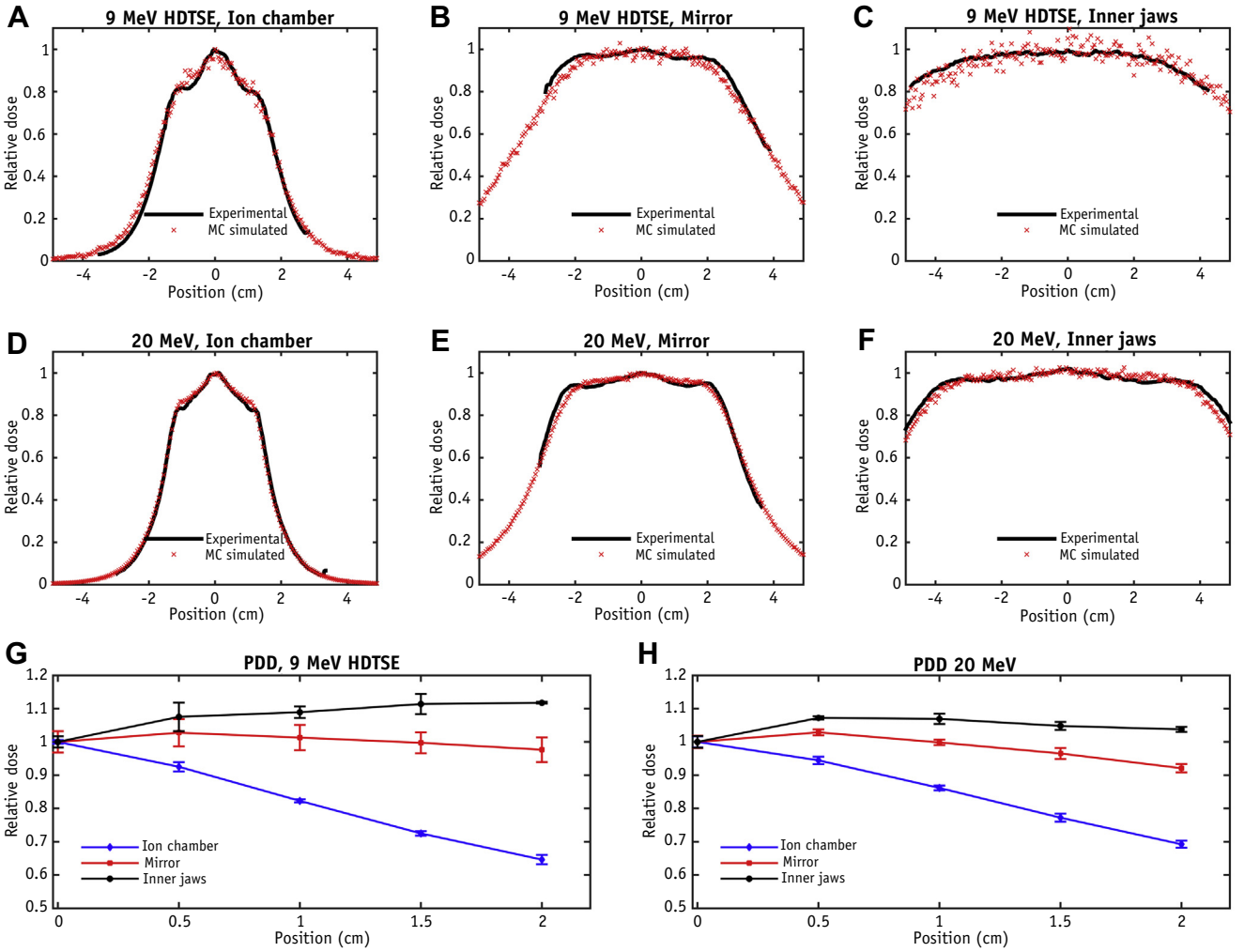

Fig. 2. Dose profiles at a 1-cm depth at the position of the ion chamber (A, D), mirror (B, E), and inner jaws (C, F) for 9- and 20-MeV electron beams. Experimental data are shown as a solid black line, and the Monte Carlo simulation are shown in red. Also shown is the measured percentage depth doses (PDDs) at the different positions for the 9- and 20-MeV electron beams (G, H). The position of the mirror provided the highest dose rate for a practically usable field size and depth dose for small animal experiments. *Abbreviation:* HDTSE = high dose total skin electron. (A color version of this figure is available at www.redjournal.org.)

thorax irradiation, a dose falloff of ~13% at a depth of 2 cm compared with entrance dose was found. For the brain, a dose falloff of ~21% was found.

Tuned field characteristics

After tuning, the dose profiles at all positions were found to be slightly asymmetric (Fig. 5), with ±3% variation across the field. No change in the PDD was found between the pre- and post-tuning states. The dose rates measured increased by a factor of 13 and 40 after tuning compared with the 9- and 20-MeV pretuning beams, respectively. The measured average dose rates at 1-cm depth varied from 900 Gy/s at the position of the ion chamber to 70 Gy/s at the position of the inner jaws. No statistically significant change in field size was found between the pre- and post-tuning states.

Discussion

Here we present a methodologic approach for using a clinical LINAC for FLASH irradiation of small animals. In our approach, we used a Varian Clinac 21EX (Varian Medical Systems) and evaluated field characteristics at different positions, with and without tuning, to find the optimal position in terms of field size, dose rate, and dose falloff. The dosimetric characterization in the present study was performed with Gafchromic EBT2 film, which has previously been shown to be practically independent of energy in the range of 1 to 100 MeV and dose rate

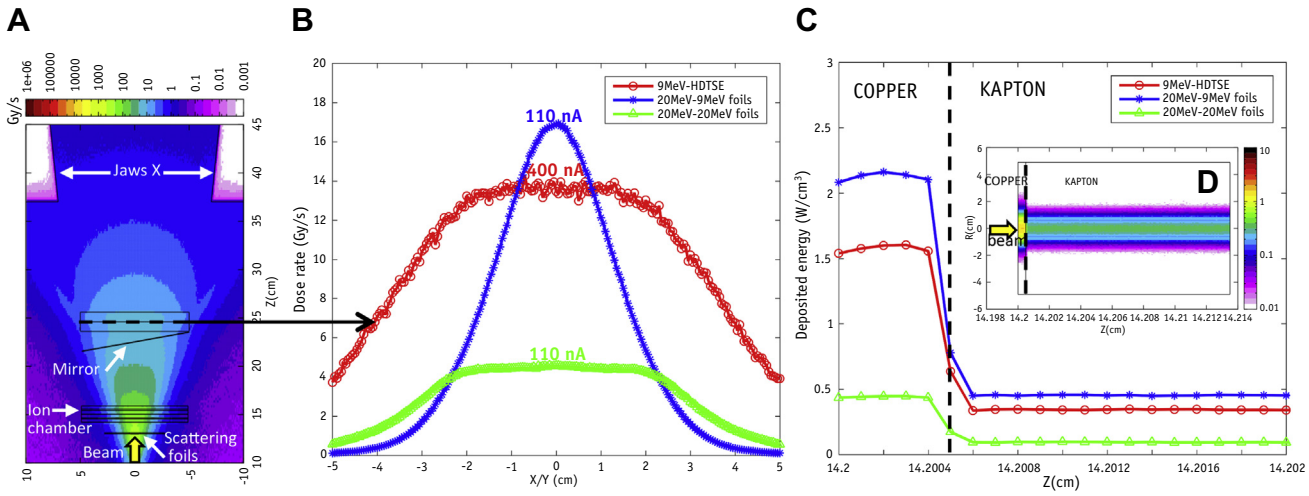

Fig. 3. Dose rate map (A) and dose rate profiles (B) at the position of the mirror for the 9-MeV high dose total skin electron (HDTSE) beam, 20-MeV beam, and 20-MeV beam with scattering foils for the 9-MeV HDTSE beam. The beam currents for each energy mode are indicated on the profile curves. (C) Energy deposition profiles in the copper and Kapton layers for a total thickness of 135 μm at the entrance window of the ion chamber for the same energies and beam currents. (D) Energy deposition map for the 9-MeV HDTSE beam. The central axis dose rate could be increased without significantly affecting the energy deposition in the ion chamber components using the 9-MeV scattering foil with the 20-MeV beam. However, achieving a higher dose rate for a practical field size requires increasing the beam current rather than decreasing the scattering.

$\leq 9.0 \times 10^{12}$ Gy/s (the maximum dose rate per pulse in the present study was 1.7×10^{6} Gy/s) (18-20).

Electrons are preferred to photons in the present setup for several reasons. First, the depth dose profile for electrons is superior to photons in small animal irradiation when using single beam irradiations. At standard conditions (ie, SSD at 100 cm with a 10 × 10 field), photons in the megavoltage range show a very steep dose build-up up to the dose maximum at around a 3-cm depth (21). This would result in a heterogeneous dose distribution in the irradiated mouse if bolus material were not applied. In contrast, for electrons, the entrance dose is at ~85% and >95% of the dose maximum for 9- and 20-MeV electrons, respectively (21, 22). This allows for a more homogeneous dose distribution when irradiating small animals. Furthermore, with the very short SSD in the current setup, the dose buildup effect becomes less important compared with the inverse square effect, especially at the position of the ion chamber. Second, it was assumed that the tuning process when using electrons would result in a greater dose rate compared with using photons owing to the large loss of charge in the target in photon mode (23). The tuning process was limited to the 20-MeV beam because of the improved depth dose characteristics in small fields with higher energy (24, 25).

The usable field size, in the present report defined as the area receiving >90% of the maximum dose, increased with the increased distance from the virtual source. At the position of the ion chamber, the usable field size was ~1 cm in diameter for the 2 energies, which had increased to >7 cm at the position of the inner jaws. For small animal (mouse) applications, a field size of 1 cm will allow for single organ irradiation. However, at the position of the ion chamber, a very strong dose falloff with depth was found, primarily due to the close proximity to the virtual source of the LINAC. This would result in a dose falloff of >30% over a distance of 2 cm. Therefore, the position of the mirror might be considered a reasonable compromise for animal irradiation owing to the tradeoff between the size of the usable field, dose rate, and dose falloff with depth.

A potential strategy to increase the dose rate is to use different scattering foils for different energies than what is normally used clinically. For each energy, a different set of thin foils is used to scatter and shape the beam: the foils are made of aluminum and tantalum, with thicknesses ranging from tens of microns to 1 mm. The possibility of using thinner scattering foils for the highest energy (ie, 20 MeV) was explored, and the results showed that an increase of >300% could be achieved without seriously increasing the energy deposited in highly valued components such as the ion chamber. However, this increase in dose rate would come at the cost of the field size. Thus, the field size at 90% of the maximum dose decreases from 5 cm to <2 cm, restricting the possible use of this beam setup for larger organ irradiation.

The procedure to achieve the higher dose rate was ultimately performed by increasing the gun current and the radiofrequency power, together with identifying the location in the head of the machine, to provide the optimal combination of dose rate and dose homogeneity across practical field sizes and depths. Owing to the saturation effects in the ion chamber, the delivered dose could not be controlled reliably using monitor units, and an Arduino Uno microcontroller was

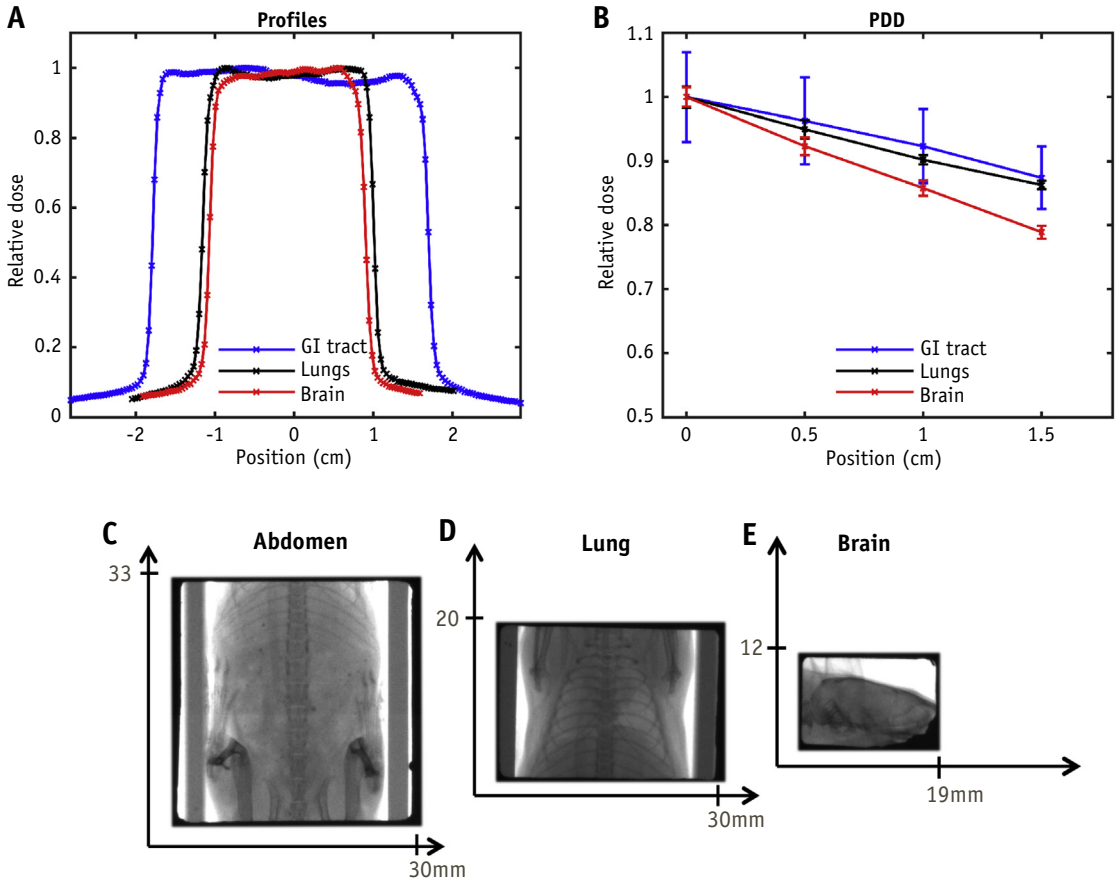

Fig. 4. (A) Dose profiles at 1-cm depth, (B) percentage depth doses (PDDs) when applying organ-specific shielding, (C) field projection for abdomen irradiation (33 × 30-mm field), (D) field projection for thorax irradiation (20 × 30-mm field), and (E) field projection for brain irradiation (12 × 19-mm field). Flat profiles were achieved for all 3 shielding situations, with PDDs showing about a 10% decrease in dose at 1.5-cm depth compared with surface dose for the abdomen and thorax fields. Stronger dose falloff was observed for the brain field. *Abbreviation:* GI = gastrointestinal.

constructed and connected to the gating interface. The microcontroller was programmed to open or close a dry-reed relay to switch the gating control on and off. The internal clock of the Arduino board has a frequency of 16 MHz, and the timing accuracy of the Arduino board was tested with an oscilloscope. It was found that the header pin toggle was on the scale of a few microseconds. The limiting case of beam shutoff was the switching time of toggling the dry-reed relay, and this was measured to be ~1 ms, much shorter than the minimum time between pulses (5.5 ms; Table E2; available at www.redjournal.org). However, because of the gating interface behavior, it was observed that the dose measured during a fixed timing interval could vary. A small difference was attributed to having an extra pulse let through (the LINAC polling clock for gating the beam could be out of sync with the gating interface being switched open, thus allowing an extra pulse to be emitted). It was also observed that the initial pulses generated after beaming on varied in size (dose/pulse) and that "full" pulses were produced only after 2 to 4 pulses had been delivered. This variation was attributed to the nature of the feedback mechanism associated with the automatic frequency control. Therefore, the overall uncertainty in dose delivery correlated almost exclusively with the individual dose per pulse error of the machine.

To the best of our knowledge, only 2 other research groups are studying FLASH small animal irradiation using custom experimental LINACs able to deliver dose rates of >50 Gy/s (9, 26, 27). Similar to our proposed system, these systems also use electrons but with an energy range of 4.5 to 6 MeV. In our system, using 20-MeV electrons, we found a very low dependence of absorbed dose with depth, providing the advantage of a more homogeneous dose in the irradiated small animal compared with lower beam energies.

A number of features can be implemented to further increase the reproducibility of the dose delivery. In the current setup, an Arduino board, connected to the gating interface, was used instead of the built-in ion chamber owing to the recombination effects therein. This allowed us to have reproducibility of ±1 pulse due to internal uncertainties and the lag time of the gating control. The implementation of a toroid with real-time measurements of the electron beam before exposure of the small animal would allow for a quick read out of the beam charge, and

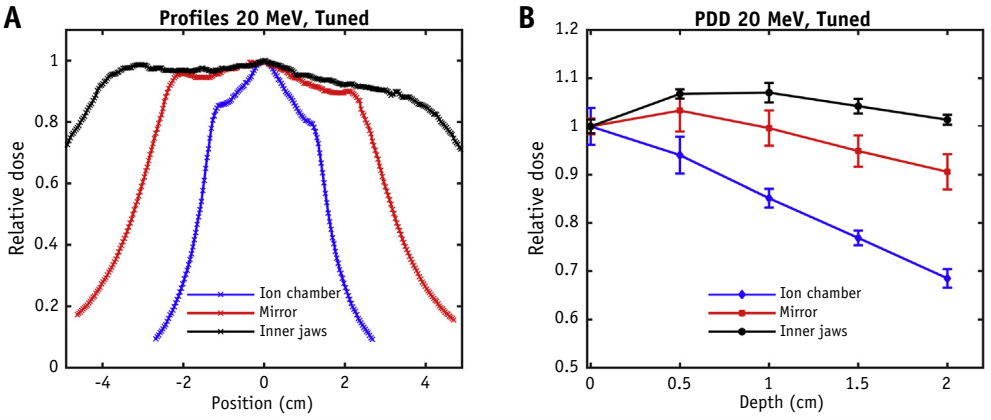

C

Position	Energy	Average dose rate (Gy/s)	Instantaneous dose rate* (Gy/s)	Field diameter 90% (mm)	Field diameter 50% (mm)
Ion chamber	20 MeV (tuned)	900±20	1700000±37000	12±0.23	33±0.17
Mirror	20 MeV (tuned)	220±8.0	410000±15000	41±3.3	65±0.17
Inner jaws	20 MeV (tuned)	70±1.5	130000±2700	69±3.9	-(-)

*Instantaneous dose rate based on measured average dose rate, with 5μs pulse length (108 Hz)

Fig. 5. (A) Dose profiles at 1-cm depth, (B) percentage depth doses (PDDs) at different positions, and (C) measured dose rates and field dimensions at 1-cm depth after tuning of linear accelerator, together with the standard deviation of the measured values. A minor asymmetric profile was observed after tuning owing to failure to update the steering coil settings between the clinical and tuned state. The maximum dose rate of 900 Gy/s was observed at a 1-cm depth at the position of the ion chamber. The dose rate was 220 Gy/s at the position of the mirror, at which the field size and PDD were most relevant for small animal irradiation experiments.

the beam off could be controlled using a microcontroller directly connected to the LINAC control computer.

Conclusions

The field of ultra-high dose rate radiobiology is still in its infancy; however, recent preclinical data showing a reduction of normal tissue toxicity but maintaining the same tumor cell killing per dose could revolutionize the field of radiation oncology when ultimately translated to human treatment, the technology for which we are also developing (28, 29). However, the ability to study the biologic response to FLASH radiation therapy has been limited by the lack of availability of experimental machines to deliver dose rates >50 Gy/s. Through the proposed method, preclinical research in the field of FLASH can become available to a broader research community, given the more general accessibility of clinical LINACs. The method requires only relatively simple modifications to a clinical LINAC and results in practically usable dose rates exceeding 200 Gy/s without extended down times from clinical service.

References

1. Lohse I, Lang S, Hrbacek J, et al. Effect of high dose per pulse flattening filter-free beams on cancer cell survival. *Radiother Oncol* 2011;101:226-232.
2. Ling CC, Gerweck LE, Zaider M, et al. Dose-rate effects in external beam radiotherapy redux. *Radiother Oncol* 2010;95:261-268.
3. Ponette V, Le Péchoux C, Deniaud-Alexandre E, et al. Hyperfast, early cell response to ionizing radiation. *Int J Radiat Biol* 2000;76:1233-1243.
4. Auer S, Hable V, Greubel C, et al. Survival of tumor cells after proton irradiation with ultra-high dose rates. *Radiat Oncol* 2011;6:139.
5. Zlobinskaya O, Siebenwirth C, Greubel C, et al. The effects of ultra-high dose rate proton irradiation on growth delay in the treatment of human tumor xenografts in nude mice. *Radiat Res* 2014;181:177-183.
6. Matsuura T, Egashira Y, Nishio T, et al. Apparent absence of a proton beam dose rate effect and possible differences in RBE between Bragg peak and plateau. *Med Phys* 2010;37:5376-5381.
7. Rafat M, Bazalova M, Palma B, et al. SU-C-BRE-06: Radiobiological advantage of very rapid irradiation. *Med Phys* 2014;41:95.
8. Rafat M, Bazalova M, Palma BA, et al. Impact of very rapid irradiation on clonogenic survival. *Int J Radiat Oncol Biol Phys* 2014;90:S790.
9. Favaudon V, Caplier L, Monceau V, et al. Ultrahigh dose-rate flash irradiation increases the differential response between normal and tumor tissue in mice. *Sci Transl Med* 2014;6:245ra293.
10. Stojadinovic S, Low D, Hope A, et al. MicroRT—Small animal conformal irradiator. *Med Phys* 2007;34:4706-4716.
11. Tryggestad E, Armour E, Deng H, et al. WE-D-330A-08: The small-animal radiation research platform (SARRP): Commissioning a 225 kvp "small-field" x-ray source for Monte Carlo-based treatment planning. *Med Phys* 2006;33:2241.
12. Jaffray D, Moseley D, Chow J, et al. WE-D-330A-09: An image-guided irradiator for pre-clinical radiation therapy studies. *Med Phys* 2006;33:2241.
13. Kiehl EL, Stojadinovic S, Malinowski KT, et al. Feasibility of small animal cranial irradiation with the microRT system. *Med Phys* 2008;35:4735-4743.
14. Chao T, Chen A, Tu S, et al. The evaluation of 6 and 18 mev electron beams for small animal irradiation. *Phys Med Biol* 2009;54:5847-5860.
15. Böhlen T, Cerutti F, Chin M, et al. The FLUKA code: Developments and challenges for high energy and medical applications. *Nucl Data Sheets* 2014;120:211-214.

16. Ferrari A, Sala PR, Fasso A, et al. FLUKA: A Multi-particle Transport Code (Program Version 2005). No. INFN-TC-05-11, http://citeseerx.ist.psu.edu/viewdoc/download;jsessionid=EEB379B96D692F53208B11E730545256?doi=10.1.1.393.4720&rep=rep1&type=pdf. Accessed June, 2015.
17. Thebaut J. Measurement Driven, Electron Beam Modeling and Commissioning for a Monte Carlo Treatment Planning System With Improved Accuracy. Montreél, Québec Canada: McGill Library and Collections; 2009. Available at: http://digitool.Library.McGill.CA:80/R/-?func=dbin-jump-full&object_id=67026&silo_library=GEN01. Accessed June 2015.
18. Chiu-Tsao ST, Ho Y, Shankar R, et al. Energy dependence of response of new high sensitivity radiochromic films for megavoltage and kilovoltage radiation energies. *Med Phys* 2005;32:3350-3354.
19. Arjomandy B, Tailor R, Anand A, et al. Energy dependence and dose response of Gafchromic EBT2 film over a wide range of photon, electron, and proton beam energies. *Med Phys* 2010;37:1942-1947.
20. Bazalova-Carter M, Liu M, Palma B, et al. Comparison of film measurements and Monte Carlo simulations of dose delivered with very high-energy electron beams in a polystyrene phantom. *Med Phys* 2015;42:1606-1613.
21. Podgorsak EB. Radiation Physics for Medical Physicists, 2nd ed. In: Greenbaum E, Aizawa M, Andersen OS, et al., editors. Biological and Medical Physics Biomedical Engineering. Berlin: Springer-Verlag; 2010.
22. Ding GX. Energy spectra, angular spread, fluence profiles and dose distributions of 6 and 18 mv photon beams: Results of Monte Carlo simulations for a Varian 2100EX accelerator. *Phys Med Biol* 2002;47:1025-1046.
23. Siebers JV, Keall PJ, Libby B, et al. Comparison of EGS4 and MCNP4B Monte Carlo codes for generation of photon phase space distributions for a Varian 2100C. *Phys Med Biol* 1999;44:3009-3026.
24. Rustgi SN, Working KR. Dosimetry of small field electron beams. *Med Dosim* 1992;17:107-110.
25. Rashid H, Islam MK, Gaballa H, et al. Small-field electron dosimetry for the Philips SL25 linear accelerator. *Med Phys* 1990;17:710-714.
26. Favaudon V, Tourbez H, Houee-Levin C, et al. Co2.- radical induced cleavage of disulfide bonds in proteins: A gamma-ray and pulse radiolysis mechanistic investigation. *Biochemistry* 1990;29:10978-10989.
27. Petersson K, Jaccard M, Vozenin M, et al. Dosimetry of ultra high dose rate irradiation for studies on the biological effect induced in normal brain and GBM. *Radiother Oncol* 2016;118:S84.
28. Bazalova-Carter M, Qu B, Palma B, et al. Treatment planning for radiotherapy with very high-energy electron beams and comparison of VHEE and VMAT plans. *Med Phys* 2015;42:2615-2625.
29. Palma B, Bazalova-Carter M, Hardemark B, et al. Assessment of the quality of very high-energy electron radiotherapy planning. *Radiother Oncol* 2016;119:154-158.